

This copy is for your personal, non-commercial use only.

If you wish to distribute this article to others, you can order high-quality copies for your colleagues, clients, or customers by [clicking here](#).

Permission to republish or repurpose articles or portions of articles can be obtained by following the guidelines [here](#).

The following resources related to this article are available online at www.sciencemag.org (this information is current as of October 7, 2010):

Updated information and services, including high-resolution figures, can be found in the online version of this article at:

<http://www.sciencemag.org/cgi/content/full/329/5999/1667>

Supporting Online Material can be found at:

<http://www.sciencemag.org/cgi/content/full/329/5999/1667/DC1>

This article **cites 27 articles**, 4 of which can be accessed for free:

<http://www.sciencemag.org/cgi/content/full/329/5999/1667#otherarticles>

This article appears in the following **subject collections**:

Immunology

<http://www.sciencemag.org/cgi/collection/immunology>

We found that α -synuclein directly promotes SNARE-complex assembly through a nonenzymatic mechanism that involves simultaneous binding of α -synuclein to phospholipids via its N terminus and to synaptobrevin-2 via its C terminus (fig. S12). The SNARE complex-promoting function of α -synuclein becomes important during increased synaptic activity and aging, rendering its action akin to a proofreading activity that is essential for the continued maintenance of SNARE-mediated fusion over the lifetime of an animal. As a result, loss of synuclein function manifests in an age-dependent loss of neuronal function, as revealed in $\alpha\beta$ -synuclein TKO mice whose phenotype resembles the delayed onset and slow progression of a neurodegenerative disease. Relative loss of α -synuclein function, for example by sequestration of α -synuclein in Lewy bodies or by increased truncation of α -synuclein during aging (23–27), may thus contribute to neurodegenerative diseases such as Parkinson's disease and Lewy body dementia. Furthermore, the increase in γ -synuclein in many cancers (12) may support enhanced membrane traffic in transformed cells.

References and Notes

1. S. Martens, H. T. McMahon, *Nat. Rev. Mol. Cell Biol.* **9**, 543 (2008).
2. W. Wickner, R. Schekman, *Nat. Struct. Mol. Biol.* **15**, 658 (2008).
3. T. C. Südhof, J. E. Rothman, *Science* **23**, 474 (2009).
4. M. L. Kramer, W. J. Schulz-Schaeffer, *J. Neurosci.* **27**, 1405 (2007).
5. S. W. Scheff, D. A. Price, F. A. Schmitt, S. T. DeKosky, E. J. Mufson, *Neurology* **68**, 1501 (2007).
6. B. C. Gray, Z. Siskova, V. H. Perry, V. O'Connor, *Neurobiol. Dis.* **35**, 63 (2009).
7. R. Fernández-Chacón *et al.*, *Neuron* **42**, 237 (2004).
8. D. F. Clayton, J. M. George, *Trends Neurosci.* **21**, 249 (1998).
9. M. H. Polymeropoulos *et al.*, *Science* **276**, 2045 (1997).
10. M. G. Spillantini *et al.*, *Nature* **388**, 839 (1997).
11. A. Gupta, V. L. Dawson, T. M. Dawson, *Ann. Neurol.* **64** (suppl. 2), S3 (2008).
12. M. Ahmad, S. Attoub, M. N. Singh, F. L. Martin, O. M. El-Agnaf, *FASEB J.* **21**, 3419 (2007).
13. S. Liu *et al.*, *EMBO J.* **23**, 4506 (2004).
14. V. M. Nemani *et al.*, *Neuron* **65**, 66 (2010).
15. S. Chandra, G. Gallardo, R. Fernández-Chacón, O. M. Schlüter, T. C. Südhof, *Cell* **123**, 383 (2005).
16. Materials and methods are available as supporting material on Science Online.
17. S. Chandra, X. Chen, J. Rizo, R. Jahn, T. C. Südhof, *J. Biol. Chem.* **278**, 15313 (2003).
18. P. García-Junco-Clemente *et al.*, *J. Neurosci.* **30**, 7377 (2010).
19. T. Hayashi *et al.*, *EMBO J.* **13**, 5051 (1994).
20. A. Abeliovich *et al.*, *Neuron* **25**, 239 (2000).
21. S. Chandra *et al.*, *Proc. Natl. Acad. Sci. U.S.A.* **101**, 14966 (2004).
22. N. Ninkina *et al.*, *Mol. Cell. Biol.* **23**, 8233 (2003).
23. M. G. Spillantini *et al.*, *Nature* **388**, 839 (1997).
24. A. Takeda *et al.*, *Am. J. Pathol.* **152**, 367 (1998).
25. P. J. Kahle *et al.*, *Am. J. Pathol.* **159**, 2215 (2001).
26. C. W. Liu *et al.*, *J. Biol. Chem.* **280**, 22670 (2005).
27. P. K. Auluck, H. Y. Chan, J. Q. Trojanowski, V. M. Lee, N. M. Bonini, *Science* **295**, 865 (2002).
28. We thank S. Chandra for advice. This work was supported by postdoctoral fellowships from the Human Frontiers Program (LT00527/2006-L to M.S. and LT000135/2009-L to T.T.) and the Deutsche Akademie der Naturforscher Leopoldina (BMBF-LPD 9901/8-161 to J.B.).

Supporting Online Material

www.sciencemag.org/cgi/content/full/science.1195227/DC1
Materials and Methods
Figs. S1 to S12
References

16 July 2010; accepted 16 August 2010
Published online 26 August 2010;
10.1126/science.1195227
Include this information when citing this paper.

Stability of the Regulatory T Cell Lineage in Vivo

Yuri P. Rubtsov,^{1*} Rachel E. Niec,^{1*} Steven Josefowicz,¹ Li Li,² Jaime Darce,² Diane Mathis,² Christophe Benoist,² Alexander Y. Rudensky^{1†}

Tissue maintenance and homeostasis can be achieved through the replacement of dying cells by differentiating precursors or self-renewal of terminally differentiated cells or relies heavily on cellular longevity in poorly regenerating tissues. Regulatory T cells (T_{reg} cells) represent an actively dividing cell population with critical function in suppression of lethal immune-mediated inflammation. The plasticity of T_{reg} cells has been actively debated because it could factor importantly in protective immunity or autoimmunity. By using inducible labeling and tracking of T_{reg} cell fate in vivo, or transfers of highly purified T_{reg} cells, we have demonstrated notable stability of this cell population under physiologic and inflammatory conditions. Our results suggest that self-renewal of mature T_{reg} cells serves as a major mechanism of maintenance of the T_{reg} cell lineage in adult mice.

Continuous replacement of differentiated cells within some tissues, such as the gut epithelium, is achieved by their de novo generation from a pool of precursor cells (1), whereas other tissues with reduced regenerative and proliferative capacity, such as the central nervous system, largely rely on cellular longevity for maintenance. Replication and self-renewal of differentiated cells, as shown for pancreatic β -cells, represents another potential mechanism underlying tissue maintenance (2). The latter strat-

egy raises the issue of stability versus plasticity of a differentiated state, which is of particular importance for the proliferating cells of the immune system. Regulatory T cells (T_{reg} cells), defined by expression of the transcription factor Foxp3, represent a dedicated suppressor cell type whose maintenance is required throughout life to restrain fatal autoimmunity (3–7). The instability of the T_{reg} cell fate—their ability to further differentiate into diverse effector T cell (T_{eff} cell) types—remains controversial. Many T_{reg} cells express T cell receptors (TCRs) with heightened affinity for self-peptide major histocompatibility complexes (MHCs) (8–11), and ablation of a conditional Foxp3 allele in mature T_{reg} cells results in generation of “former” T_{reg} cells that are capable of causing inflammatory tissue lesions (12). Thus, the stability of Foxp3 expression under basal and inflammatory conditions is an important determinant of immune homeostasis and of im-

mediate relevance to the question of whether T_{reg} cells represent a distinct, stable cell lineage or a transient meta-stable activation state. Genetic fate mapping provides means to evaluate both lineage stability and informs mechanisms of tissue maintenance in vivo.

We used this approach to evaluate T_{reg} cell lineage stability under basal and inflammatory conditions and generated knock-in mice harboring a cassette containing an internal ribosome entry site (IRES) followed by DNA sequence encoding a “triple” fusion protein of the enhanced green fluorescent protein (eGFP) with Cre recombinase and mutated human estrogen receptor ligand-binding domain (ERT2) inserted into the 3' untranslated region (UTR) of the Foxp3 gene (13). The Foxp3^{eGFP-Cre-ERT2} mice were bred to mice that expressed a Cre recombination reporter allele of the ubiquitously expressed ROSA26 locus containing a loxP site-flanked STOP cassette followed by a DNA sequence encoding yellow fluorescent protein (YFP) (R26Y) (fig. S1). In the Foxp3^{eGFP-Cre-ERT2} × R26Y mice, the GFP-CreERT2 fusion protein is sequestered in the cytosol, and therefore YFP is not expressed; but treatment with tamoxifen allows for nuclear translocation of the fusion protein, excision of the floxed STOP cassette, and constitutive and heritable expression of YFP in a cohort of cells that expressed Foxp3 at the time of tamoxifen administration. In contrast to continuous labeling, inducible labeling of Foxp3-expressing cells with YFP avoids the constant incorporation into the labeled population of cells that transiently up-regulate Foxp3 and affords assessment of bona fide T_{reg} cell maintenance.

Foxp3^{eGFP-Cre-ERT2} × R26Y mice had normal numbers of CD4 and CD8 double- and single-positive thymocytes and CD4⁺ and CD8⁺ T cells

¹Howard Hughes Medical Institute and Immunology Program, Memorial Sloan-Kettering Cancer Center, New York, NY 10065, USA. ²Department of Pathology, Harvard Medical School, Boston, MA 02115, USA.

*These authors contributed equally to this work.

†Present address: Department of Fundamental Medicine, Moscow State University, Moscow 117192, Russian Federation.

‡To whom correspondence should be addressed. E-mail: rudenska@mskcc.org

in the secondary lymphoid organs (fig. S2). Foxp3 and the associated eGFP reporter were expressed in a manner indistinguishable from expression of the Foxp3 protein in control wild-type mice, and eGFP expression was limited to Foxp3⁺ cells (figs. S2 and S3A). YFP was not detected in eGFP⁺ cells in the absence of tamoxifen and was restricted to Foxp3⁺ cells upon tamoxifen administration (fig. S3, B and C). Treatment with tamoxifen resulted in three main populations of CD4⁺ T cells: eGFP⁺YFP⁻Foxp3⁻ “non-T_{reg}” cells, eGFP⁺YFP⁻ unlabeled Foxp3⁺ T_{reg} cells, and tagged eGFP⁺YFP⁺ Foxp3⁺ cells (fig. S4). We also observed a minor population of eGFP⁺YFP⁺ cells (<5% of YFP⁺ cells), which may represent cells that were transiently expressing Foxp3 at the time of tamoxifen exposure. Both YFP-tagged and -untagged eGFP⁺ T_{reg} cells expressed identical amounts of Foxp3 and all other T_{reg} cell phenotypic and activation markers tested thus far (figs. S4 and S5).

To evaluate long-term stability of Foxp3⁺ T_{reg} cells under basal conditions, *Foxp3*^{eGFP-Cre-ERT2} × R26Y mice were treated with tamoxifen and an-

alyzed 5 to 8 months later for Foxp3 expression in YFP⁺CD4⁺ T cells. The overwhelming majority of YFP⁺CD4⁺ T cells remained eGFP-positive in the lymph nodes, spleen, Peyer’s patches, skin, and lung up to 5 months after tamoxifen treatment (Fig. 1, A and B). This result was confirmed by means of intracellular staining for Foxp3 of fluorescence-activated cell sorter (FACS)-purified YFP⁺ cells (fig. S6). Furthermore, expression of T_{reg} cell-associated molecules was comparable between YFP⁺ and YFP⁺GFP⁺ cells (Fig. 1C and fig. S6), and production of proinflammatory cytokines was comparably low in both subsets (Fig. 1D). The minor population of eGFP⁻YFP⁺ cells observed 14 days after labeling failed to expand and in fact further decreased over time (Fig. 1, C and D). Thus, we did not observe a noticeable “conversion” of T_{reg} cells and their progeny into follicular T helper (TFH) or effector T cells or their dedifferentiation into naïve T cells under physiologic conditions.

Surprisingly, in euthymic mice the proportion of YFP⁺ T_{reg} cells among all Foxp3⁺ cells at 5 to 8 months after labeling was comparable with

that observed at 14 days despite continuous, albeit declining with age, output of thymus-derived T_{reg} cells (Fig. 1E). Furthermore, thymectomy failed to influence the proportion of YFP⁺ T_{reg} cells among Foxp3⁺ cells at these later time points (Fig. 1E), suggesting that the peripheral T_{reg} cell pool, which is characterized by a high proportion of cycling cells (fig. S7), is not only highly stable in adult mice but is largely self-sustained with a relatively minor contribution by newly generated thymic emigrants.

We next asked whether Foxp3 can be lost upon growth factor deprivation as a validation of our T_{reg} cell-fate tracking approach. Foxp3 induction and T_{reg} cell homeostasis are dependent upon interleukin-2 (IL-2) receptor signaling (14–19), and antibody-mediated blockade of IL-2 or IL-2R causes contraction of the T_{reg} cell population (16). Thus, we sought to explore whether IL-2 deprivation of mature T_{reg} cells is associated with death or loss of Foxp3 expression and concomitant acquisition of immune effector cytokine production. Tamoxifen-treated *Foxp3*^{eGFP-Cre-ERT2} × R26Y mice were treated

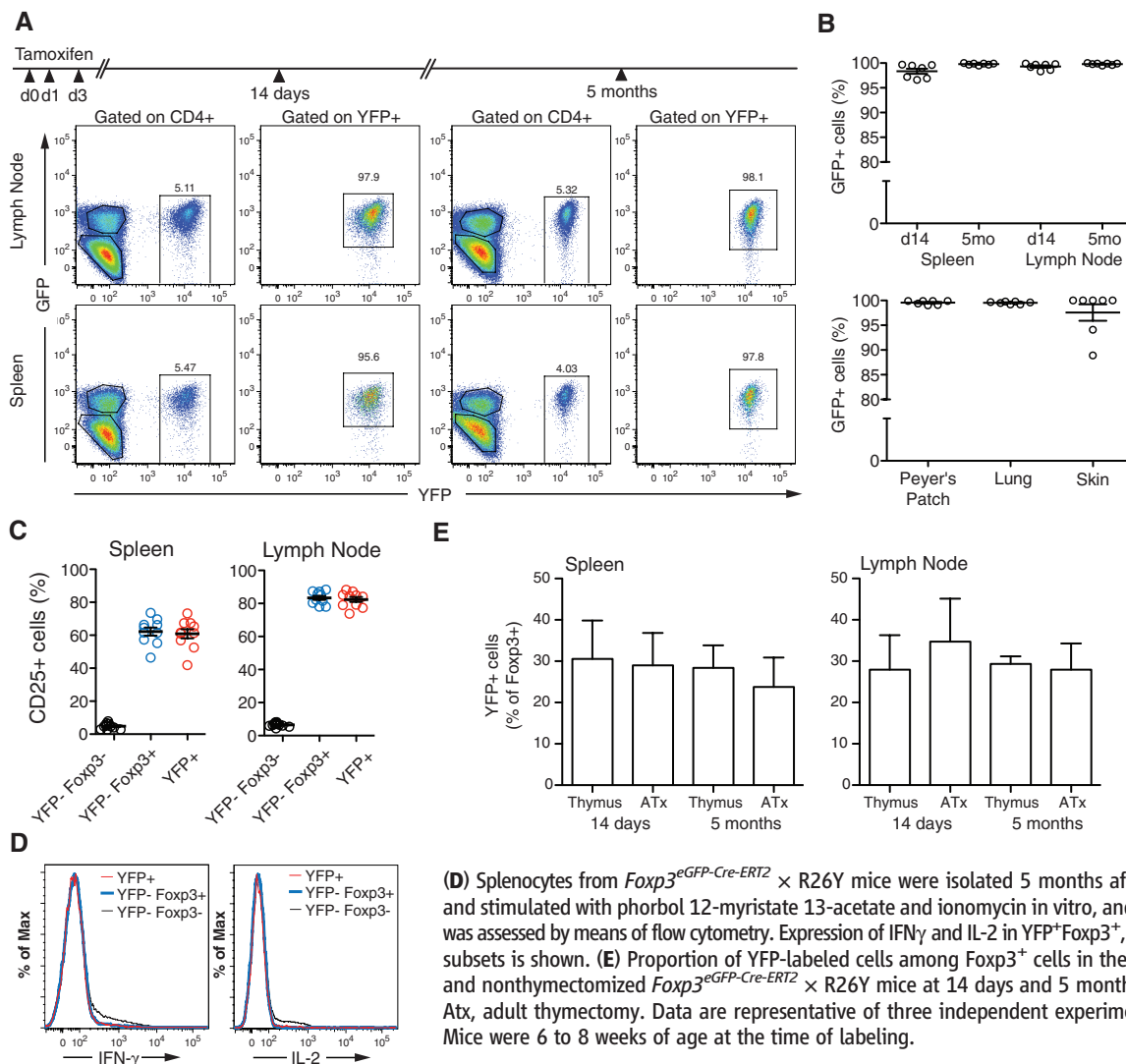


Fig. 1. Inducible labeling of Foxp3⁺ cells reveals stability of T_{reg} cell subset under physiologic conditions. (A) Representative flow-cytometric analyses demonstrate stability of Foxp3 expression at 14 days and 5 months after tamoxifen-induced labeling. YFP⁺, YFP⁺GFP⁺, and YFP⁻GFP⁻ subsets of CD4⁺ T cells and proportion of GFP⁺ cells among YFP-tagged cells are shown. Numbers represent percentages of cells within the indicated gates. (B) Percentages of YFP⁺ cells expressing GFP in the indicated organs analyzed as in (A) at 5 months after tamoxifen administration (bottom). Each symbol represents an individual mouse. (C) Flow cytometric analysis of CD25 expression in CD4⁺ cell subsets at 5 months after initial tamoxifen treatment. Expression of CD25 within the indicated subset is shown for individual mice.

(D) Splenocytes from *Foxp3*^{eGFP-Cre-ERT2} × R26Y mice were isolated 5 months after tamoxifen administration and stimulated with phorbol 12-myristate 13-acetate and ionomycin in vitro, and production of IFN γ and IL-2 was assessed by means of flow cytometry. Expression of IFN γ and IL-2 in YFP⁺Foxp3⁺, YFP⁻Foxp3⁺, and YFP⁻Foxp3⁻ subsets is shown. (E) Proportion of YFP-labeled cells among Foxp3⁺ cells in the periphery of thymectomized and nontymectomized *Foxp3*^{eGFP-Cre-ERT2} × R26Y mice at 14 days and 5 months after tamoxifen treatment. Atx, adult thymectomy. Data are representative of three independent experiments ($n \geq 3$ mice per group). Mice were 6 to 8 weeks of age at the time of labeling.

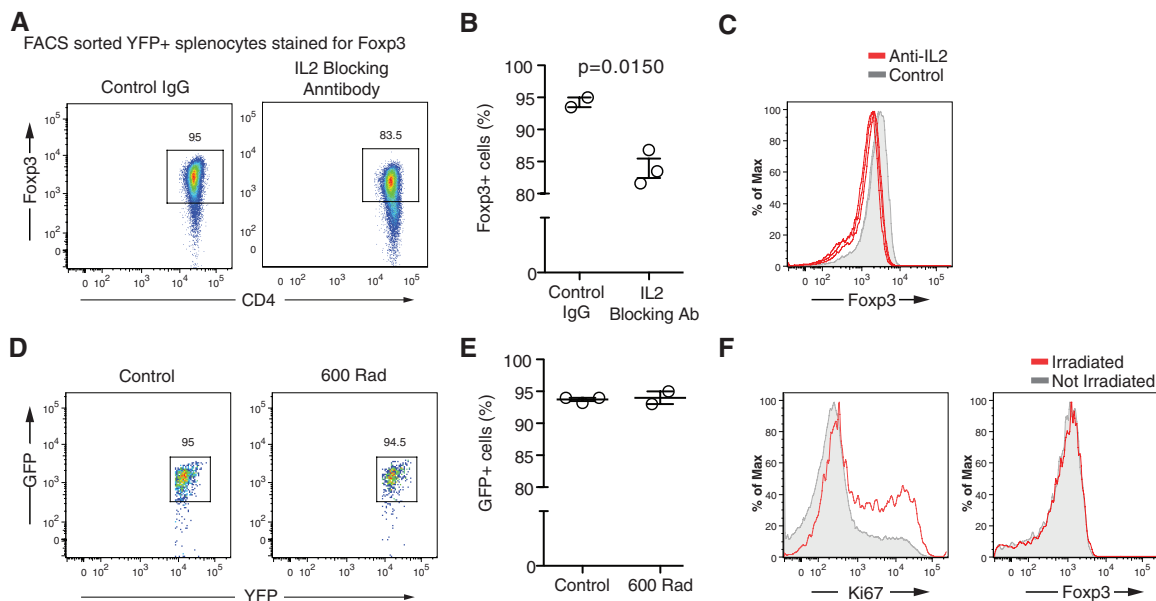
with IL-2-neutralizing antibody. IL-2 deprivation resulted in a ~30% decrease in total Foxp3⁺ T_{reg} cell numbers and a modest decrease in Foxp3 protein amounts at the single-cell level (Fig. 2, A to C). Moreover, a small subset of YFP⁺ cells was completely devoid of Foxp3. We did not, however, observe derepression of proinflammatory cytokines [interferon-γ (IFNγ), IL-17, IL-2, and tumor necrosis factor-α (TNFα)] by YFP⁺, YFP⁻GFP⁺ T_{reg} cells with decreased Foxp3 levels, or eGFP YFP⁺ cells which had lost

Foxp3 expression (fig. S8). These results demonstrate that upon IL-2 deprivation, the bulk of T_{reg} cells maintained Foxp3 expression albeit at a moderately decreased level, yet sufficient to prevent acquisition of an effector cell phenotype. Nevertheless, it is possible that IL-2 deprivation under conditions of overwhelming infection might result in a loss of Foxp3 in some T_{reg} cells (20).

Lymphopenia may also facilitate loss of Foxp3 expression in expanding T_{reg} cells. Despite use of purified T_{reg} cells in previously published

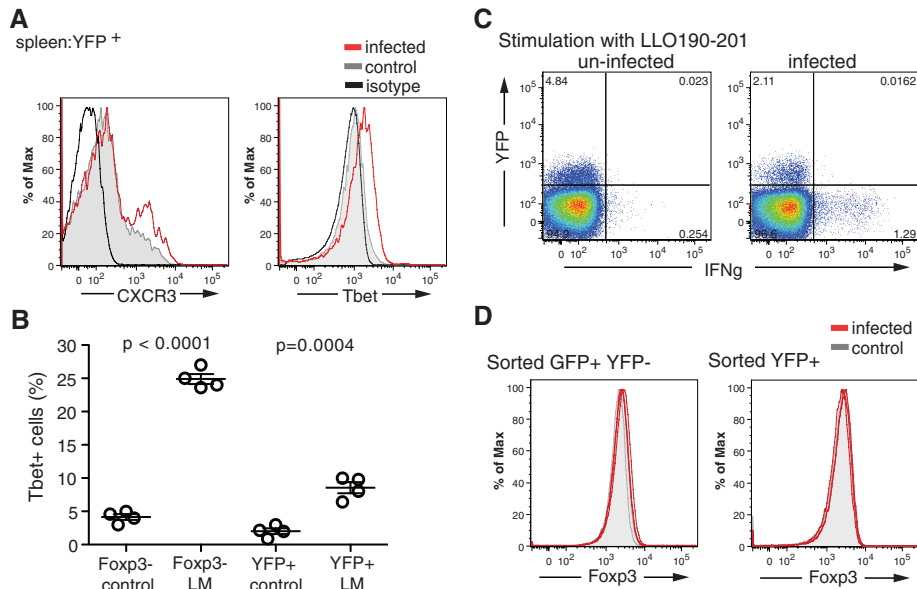
transfer studies, the possibility of outgrowth of a small number of contaminating non-T_{reg} cells and stress associated with cell transfer remain potential caveats in interpretation of these results. To circumvent these issues, we used sublethal irradiation to evaluate stability of Foxp3 expression under lymphopenic conditions. Tamoxifen-treated Foxp3^{eGFP-Cre-ERT2} × R26Y mice were irradiated (6 Gy), and the proportion of eGFP⁺ and Foxp3⁺ cells among YFP⁺CD4⁺ T cells was evaluated 14 days after irradiation. De-

Fig. 2. IL-2 deprivation results in a small but detectable decrease in Foxp3 expression. **(A to C)** Tamoxifen-treated Foxp3^{eGFP-Cre-ERT2} × R26Y mice were injected with IL-2-blocking antibody or control immunoglobulin G (IgG), and Foxp3 expression in FACS-sorted YFP⁺ cells was assessed 9 days later. **(A)** Intracellular Foxp3 staining of splenic YFP⁺ cells. Numbers represent percentages of cells in the indicated gate. **(B)** Percentages of YFP⁺ cells expressing Foxp3. Each symbol represents an individual mouse. **(C)** Relative expression of Foxp3 in YFP⁺ cells from spleens of mice treated with IL-2-blocking antibody. Data are representative of three independent experiments ($n \geq 2$ mice per group). Mice were 6 to 8 weeks of age at the time of antibody administration. **(D to F)** T_{reg} cells maintain stable expression of Foxp3 under lymphopenic conditions. Lymphopenia was induced in tamoxifen-treated Foxp3^{eGFP-Cre-ERT2} × R26Y mice upon irradiation (6 Gy), and mice were analyzed 14 days later. **(D)** Representative flow-cytometric analysis of Foxp3 expression among cells isolated from spleens of control and irradiated mice 14



days after irradiation. Numbers represent percentages of cells in the indicated gate. **(E)** Percentages of GFP⁺ cells among YFP⁺ cells in spleens 14 days after irradiation. Each symbol represents an individual mouse. **(F)** Representative flow-cytometric analysis of Foxp3 and Ki67 expression by YFP⁺ splenocytes on day 14 after irradiation. Similar data were obtained from cells isolated from lymph nodes of irradiated mice. Data are representative of ≥ 2 independent experiments, each with ≥ 2 mice per group. Mice were 8 to 12 weeks of age at the time of irradiation.

Fig. 3. Th1-type inflammation does not induce loss of Foxp3. Tamoxifen-treated Foxp3^{eGFP-Cre-ERT2} × R26Y mice were infected intravenously with 5×10^3 colony-forming units (CFU) of *Listeria monocytogenes* and analyzed 9 days later. **(A)** Flow-cytometric analysis demonstrates up-regulation of T-bet and CXCR3 by splenic YFP⁺CD4⁺ cells in infected mice. **(B)** Percent of T-bet positive cells among Foxp3⁺ and YFP⁺ splenocytes as determined in (A). Each symbol represents an individual mouse. **(C)** Antigen-specific production of IFNγ in splenocytes restimulated with LLO190-201 peptide. CD4⁺ T cell gate is shown; numbers represent percentages of cells in corresponding quadrants. **(D)** Foxp3 expression in sorted (top) YFP⁻GFP⁺ or (bottom) YFP⁺ cells from *L. monocytogenes* infected or control mice 9 days after infection. Data are representative of three independent experiments with ≥ 2 mice per group each. Mice were 6 to 8 weeks of age at the time of infection.



spite a marked increase in numbers of dividing T_{reg} cells reflected in heightened expression of Ki67 in YFP^+ and $YFP^- T_{reg}$ cells, GFP and Foxp3 expression was preserved in YFP^+ cells (Fig. 2, D to F). We considered that perturbation of the 3'UTR in $Foxp3^{eGFP-Cre-ERT2} \times R26Y$ mice may have resulted in increased Foxp3 mRNA or protein stability. However, Foxp3 mRNA decay in the presence of actinomycin D in T_{reg} cells from $Foxp3^{eGFP-Cre-ERT2} \times R26Y$ mice was more pronounced than that in T_{reg} cells from the previously described $Foxp3^{GFP}$ mice, in which GFP sequence was inserted into the 5' end of the Foxp3 coding sequence, leaving the 3'UTR intact (fig. S9) (4). To compare the stability of Foxp3 protein expression in T_{reg} cells from $Foxp3^{eGFP-Cre-ERT2} \times R26Y$ mice with that in $Foxp3^{GFP}$ mice in vivo, $CD4^+GFP^+$ cells were doubly purified by means of FACS from each mouse strain and cotransferred with $Ly5.1^+CD4^+$ T cells into TCR $\beta\delta$ -deficient mice. Three weeks after transfer, the majority (~90%) of $CD4^+Ly5.2^+$ cells maintained GFP and Foxp3 protein expression, and their percentages among cells transferred from both mouse strains were similar (fig. S10), further supporting the stability of the T_{reg} cell lineage and indicating that the modification of the 3'UTR in $Foxp3^{eGFP-Cre-ERT2} \times R26Y$ mice cannot account for this observation.

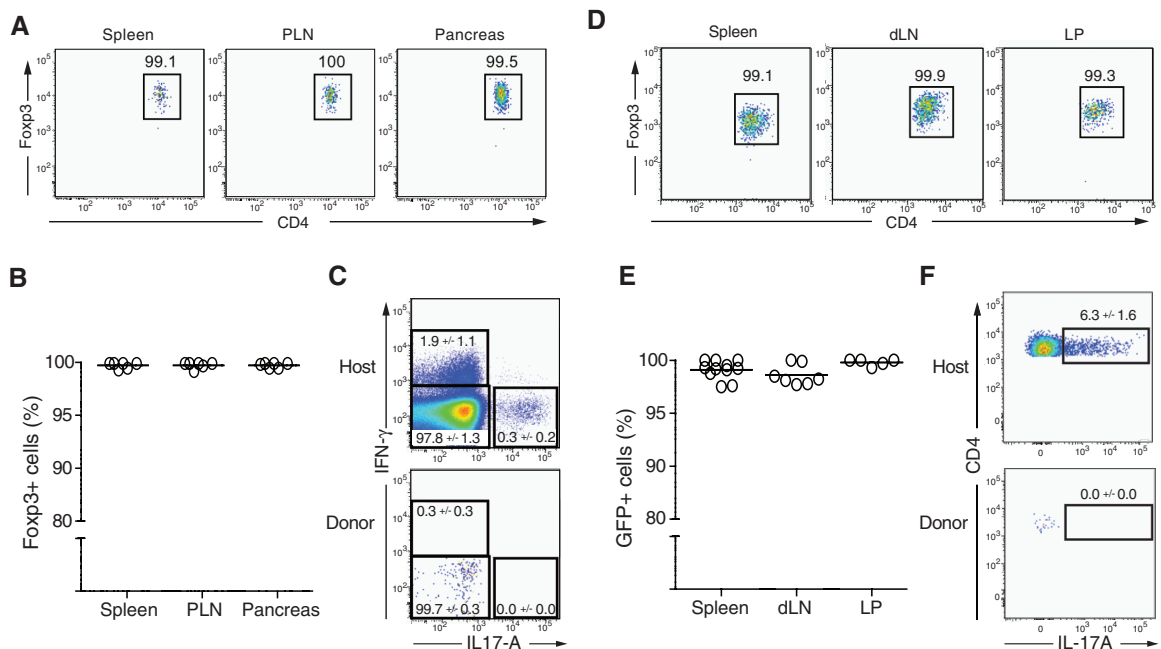
Previous studies suggested that during infection, exposure of T_{reg} cells to pro-inflammatory cytokines results in a loss of Foxp3 expression and T_{reg} cell conversion into effector T cells and was interpreted as a means to facilitate appro-

priate immune responsiveness (21). To examine the fate of $Foxp3^+ T_{reg}$ cells during infection, $Foxp3^{eGFP-Cre-ERT2} \times R26Y$ mice were treated with tamoxifen, infected with a sublethal dose of *Listeria monocytogenes*, and analyzed for T_{reg} cell stability at the peak of the immune response. After infection, we observed considerable up-regulation of the T helper 1 transcription factor T-bet and CXCR3 in $Foxp3^-$, $Foxp3^+$, and $YFP^+ CD4^+$ cells (Fig. 3, A and B, and fig. S11) and $IFN\gamma$ production by effector $CD4^+$ T cells in response to listeriolysin O (LLO) peptide (Fig. 3C and fig. S11). Nevertheless, essentially all $YFP^+ T_{reg}$ cells maintained expression of Foxp3 (Fig. 3D), including those with increased T-bet expression. Foxp3 stability was also observed in T-bet $^+Foxp3^+$ cells generated upon induction of a strong $IFN\gamma$ -dominated Th1 inflammatory response upon antibody-mediated cross-linking of CD40 (fig. S12) (22). Cross-linking of CD40 after tamoxifen-induced labeling resulted in a marked up-regulation of T-bet and CXCR3 in $Foxp3^+$ and $Foxp3^-$ cells (fig. S12). YFP-tagged cells demonstrated increased expression of CXCR3 and T-bet but at best marginally increased $IFN\gamma$ and IL-2 production (fig. S12). Furthermore, T_{reg} cells maintained expression of Foxp3 at 14 days and up to 5 months after CD40 cross-linking (fig. S12). Thus, T_{reg} cells maintain heritable Foxp3 expression even after up-regulation of the Th1 transcription factor T-bet in the course of Th1-dependent antibacterial infection and CD40 cross-linking driven Th1 inflammatory response. T-bet and CXCR3 induction in T_{reg} cells was recently shown to facilitate their ability to restrain Th1 inflammation (22).

Lastly, to evaluate the stability of $Foxp3^+$ cells in an autoimmune inflammatory setting, highly purified pancreatic-islet-antigen-specific $GFP^+ T_{reg}$ cells from $NOD.Foxp3^{GFP}.BDC2.5$ TCR-transgenic mice (23) were transferred into prediabetic, lymphoreplete $NOD.Thy1.1$ recipients at 12 weeks of age, a time point at which pancreatic infiltration is well established. Four weeks later, donor cells were enriched in the inflamed pancreas but retained expression of Foxp3 and, in contrast to recipient effector cells, expressed no detectable IL-17 or $IFN\gamma$ (Fig. 4, A to C). In parallel experiments, T_{reg} cell stability was evaluated in the K/BxN TCR-transgenic model, in which reactivity to a ubiquitous self-antigen leads IL-17- and gut microbiota-dependent generation of arthritogenic auto-antibodies (24). Highly purified $GFP^+ T_{reg}$ cells from $K/BxN.Foxp3^{GFP}$ mice were transferred into 20-day-old K/BxN recipients—at the initiation of the very robust inflammatory process—and again remained almost exclusively $Foxp3^+$ and failed to produce IL-17 in lymphoid organs or the lamina propria (Fig. 4, D to F). Thus, T_{reg} cells maintained stable Foxp3 expression and showed no evidence of effector cytokine production under conditions of autoimmune inflammation.

In contrast to our findings, a recent study reported a marked loss of Foxp3 expression in YFP-tagged $Foxp3^+ T_{reg}$ cells in $R26Y \times Foxp3-Cre$ BAC transgenic mice and acquisition of effector function by $YFP^+Foxp3^- T$ cells (25). Likewise, upon transfer into lymphopenic recipients $Foxp3^+ T_{reg}$ cells were found to lose Foxp3 expression and differentiate into TFH cells in the

Fig. 4. Foxp3 expression is stable in T_{reg} cells during autoimmune inflammation. (A to C) Highly purified GFP^+ cells from $BDC2.5.Foxp3^{eGFP}$ mice were transferred into 12-week-old prediabetic $NOD.Thy1.1$ recipients, and the spleen, pancreatic lymph nodes (PLN), or pancreatic infiltrates were analyzed 4 weeks later. (A) Representative Foxp3 staining of $Thy1.2^+CD4^+$ donor cells. (B) Tabulation of individual mice in three independent experiments. (C) Intracellular $IFN\gamma$ and IL-17 staining of host and donor $CD4^+$ cells (numbers represent percentage of cells in the gate \pm SD; $n = 3$ to 6 mice per group). (D to F) Highly purified $CD4^+GFP^+$ cells from 20-day-old $K/BxN.Foxp3^{GFP}$ mice were transferred into age-matched $K/BxN.CD45.2$ mice. (D) Spleen, joint-draining lymph node, and small intestine lamina propria (LP) were collected from arthritic 35-day-old recipients and $CD45.1^+CD4^+$ donor cells analyzed for



Foxp3-GFP expression. (E) Tabulation of individual mice in two independent experiments. (F) Expression of IL-17a by host and donor $CD4^+$ cells from the lamina propria (numbers represent percentage of cells in the gate \pm SD; $n = 3$ mice per group). Data are representative of two independent experiments.

Peyer's patches (26). Seemingly unstable Foxp3 expression observed in these and other studies (21) can be due to cellular stress, the presence of few contaminating Foxp3⁻ cells or cells which underwent transient Foxp3 up-regulation, or recently generated Foxp3⁺ cells on their way to stable Foxp3 expression yet still able to expand and differentiate into effector T cells in lymphopenic or nonlymphopenic settings. Consistent with the latter notion, loss of Foxp3 expression by a minor population of YFP⁺ cells was observed during induction of Foxp3 in peripheral YFP⁻GFP⁻CD4⁺ T cells under lymphopenic conditions. In contrast, YFP⁺GFP⁺T_{reg} cells maintained Foxp3 expression in these experiments (fig. S13). Furthermore, transient expression of Foxp3 during retinoic acid receptor (RAR)-related orphan receptor- γ (ROR γ)-dependent differentiation of Th17 cells was visualized through activation of the R26Y allele by Cre recombinase constitutively expressed under control of the endogenous *Foxp3* locus (27). Additionally, differences in regulation of expression of *Foxp3* bacterial artificial chromosome (BAC) transgene and the endogenous *Foxp3* locus encoding Cre can also affect the discrepant outcomes of YFP-tagging of T_{reg} cells in the corresponding experimental models.

We demonstrated that the T_{reg} cell lineage is remarkably stable under physiologic conditions and after a variety of challenges. Stable

Foxp3 expression in committed T_{reg} cells is probably facilitated by a positive autoregulatory loop (28). Our results also suggest that continuous self-renewal of the established T_{reg} cell population combined with heritable maintenance of Foxp3 expression serves as a major mechanism of maintenance of this lineage in adult mice.

References and Notes

1. F. el Marjou *et al.*, *Genesis* **39**, 186 (2004).
2. Y. Dor, J. Brown, O. I. Martinez, D. A. Melton, *Nature* **429**, 41 (2004).
3. J. D. Fontenot, M. A. Gavin, A. Y. Rudensky, *Nat. Immunol.* **4**, 330 (2003).
4. J. D. Fontenot *et al.*, *Immunity* **22**, 329 (2005).
5. S. Hori, T. Takahashi, S. Sakaguchi, *Adv. Immunol.* **81**, 331 (2003).
6. R. Khatri, T. Cox, S.-A. Yasayko, F. Ramsdell, *Nat. Immunol.* **4**, 337 (2003).
7. J. M. Kim, J. P. Rasmussen, A. Y. Rudensky, *Nat. Immunol.* **8**, 191 (2007).
8. I. Apostolou, A. Sarukhan, L. Klein, H. von Boehmer, *Nat. Immunol.* **3**, 756 (2002).
9. C.-S. Hsieh *et al.*, *Immunity* **21**, 267 (2004).
10. M. S. Jordan *et al.*, *Nat. Immunol.* **2**, 301 (2001).
11. R. Pacholczyk, H. Ignatowicz, P. Kraj, L. Ignatowicz, *Immunity* **25**, 249 (2006).
12. L. M. Williams, A. Y. Rudensky, *Nat. Immunol.* **8**, 277 (2007).
13. Materials and methods are available as supporting material on Science Online.
14. W. Liao *et al.*, *Nat. Immunol.* **9**, 1288 (2008).
15. M. A. Burchill, J. Yang, C. Vogtenhuber, B. R. Blazar, M. A. Farrar, *J. Immunol.* **178**, 280 (2007).
16. R. Setoguchi, S. Hori, T. Takahashi, S. Sakaguchi, *J. Exp. Med.* **201**, 723 (2005).

17. J. D. Fontenot, J. P. Rasmussen, M. A. Gavin, A. Y. Rudensky, *Nat. Immunol.* **6**, 1142 (2005).
18. A. L. Bayer, A. Yu, T. R. Malek, *J. Immunol.* **178**, 4062 (2007).
19. T. R. Malek *et al.*, *J. Clin. Immunol.* **28**, 635 (2008).
20. G. Oldenhove *et al.*, *Immunity* **31**, 772 (2009).
21. X. Zhou, S. Bailey-Bucktrout, L. T. Jeker, J. A. Bluestone, *Curr. Opin. Immunol.* **21**, 281 (2009).
22. M. A. Koch *et al.*, *Nat. Immunol.* **10**, 595 (2009).
23. J. D. Katz, B. Wang, K. Haskins, C. Benoist, D. Mathis, *Cell* **74**, 1089 (1993).
24. H. J. Wu *et al.*, *Immunity* **32**, 815 (2010).
25. X. Zhou *et al.*, *Nat. Immunol.* **10**, 1000 (2009).
26. M. Tsuji *et al.*, *Science* **323**, 1488 (2009).
27. L. Zhou *et al.*, *Nature* **453**, 236 (2008).
28. Y. Zheng *et al.*, *Nature* **463**, 808 (2010).
29. We thank K. Forbush, T. Chu, L. Karpik, A. Bravo, J. Herlihy, P. Zarin, G. Gerard, A. Ortiz-Lopes, and K. Hattori for assistance with mouse colony management; F. Costantini for R26Y mice; V. Kuchroo for Foxp3-IRES-GFP mice; P. Chambon for Cre-ERT2 plasmid; E. Pamer, C. Shi, and E. Leiner for *L. monocytogenes* and assistance with experiments; and P. Fink and K. Simmons for cells from Rag2pGFP mice and helpful discussion. R.E.N. was supported by NIH Medical Scientist Training Program grant GM07739. A.Y.R. is an investigator with the Howard Hughes Medical Institute, and this work was also supported by grant AI51530 from the NIH to C.B. and D.M.

Supporting Online Material

www.sciencemag.org/cgi/content/full/329/5999/1667/DC1
Materials and Methods
Figs. S1 to S13

7 May 2010; accepted 2 August 2010
10.1126/science.1191996

Dendritic Discrimination of Temporal Input Sequences in Cortical Neurons

Tiago Branco, Beverley A. Clark, Michael Häusser*

The detection and discrimination of temporal sequences is fundamental to brain function and underlies perception, cognition, and motor output. By applying patterned, two-photon glutamate uncaging, we found that single dendrites of cortical pyramidal neurons exhibit sensitivity to the sequence of synaptic activation. This sensitivity is encoded by both local dendritic calcium signals and somatic depolarization, leading to sequence-selective spike output. The mechanism involves dendritic impedance gradients and nonlinear synaptic *N*-methyl-D-aspartate receptor activation and is generalizable to dendrites in different neuronal types. This enables discrimination of patterns delivered to a single dendrite, as well as patterns distributed randomly across the dendritic tree. Pyramidal cell dendrites can thus act as processing compartments for the detection of synaptic sequences, thereby implementing a fundamental cortical computation.

In sensory pathways, the relative timing of spikes from different neuronal populations can represent features of stimuli (1–4). A fundamental problem in cortical sensory processing is, thus, the discrimination of different spatiotemporal sequences of inputs (5). Although networks composed of simple neurons can, in principle, decode temporal sequences, the size

and complexity of such networks can be greatly reduced if individual neurons can perform temporal decoding (6, 7). Dendritic trees might contribute to this decoding, because they are highly nonlinear devices that can locally process and integrate synaptic signals (8–10). For example, spatiotemporally clustered inputs trigger dendritic spikes (11–15), which can generate independent functional subunits, enhancing the computational potential of the neuron (16–18) and encoding spatial and temporal input synchrony. Whether these nonlinear dendritic properties can be exploited to perform higher-order computations such as temporal sequence detection is

unknown. In 1964, Wilfrid Rall predicted that, because dendrites act as a delay line, activation of synapses along a dendrite in different directions should produce different responses at the soma (19). Although the dendrites of retinal neurons exhibit such direction selectivity (20–22), experimental investigation of the sensitivity to spatiotemporal sequences of synaptic activation in cortical pyramidal cell dendrites has been a challenge due to the difficulty in delivering the spatiotemporal input patterns with the necessary submillisecond and submicron precision.

To test the sensitivity of single dendrites to the order of activation of a defined set of synapses, we controlled spatiotemporal input patterns using multisite, two-photon glutamate uncaging at identified dendritic spines (15, 23) in layer 2/3 pyramidal neurons of somatosensory and visual cortex. We first studied the sensitivity of single dendrites to an ordered sequence of synaptic activation in opposite directions, selecting 8 to 10 spines on single basal and apical oblique dendritic branches (Fig. 1, A and B). Activating each site in isolation (Fig. 1C) produced synaptic responses [glutamate excitatory postsynaptic potentials (gluEPSPs)] within physiological parameters (fig. S1). Sequential activation of spines from the dendritic branch to the soma (IN) or from the soma to the tip (OUT) produced strongly directionally sensitive responses. The IN direction always produced a larger somatic response than the OUT direction (Fig. 1, D and E) ($31 \pm 4\%$ increase, $P < 0.0001$,

Wolfson Institute for Biomedical Research and Department of Neuroscience, Physiology, and Pharmacology, University College London, Gower Street, London WC1E 6BT, UK.

*To whom correspondence should be addressed. E-mail: m.hauser@ucl.ac.uk